PCCP

Accepted Manuscript

ROYAL SOCIETY OF CHEMISTRY

www.rsc.org/pccp

Mechanistic and Kinetic Implications on ORR at Au(100) Electrode, pH, Temperature and H-D kinetic Isotope effects

Dong Mei, Zheng Da He, Yong Li Zheng, Dao Chuan Jiang, Yan-Xia Chen*

Hefei National Laboratory for Physical Sciences at Microscale, Department of Chemical Physics, University of Science and Technology of China, Hefei, 230026, China

yachen@ustc.edu.cn

Tel / Fax: +86-551-3600035

Abstract： pH, temperature and H-D kinetic isotope effects (KIEs) on ORR at Au(100) has been examined systematically using hanging meniscus rotating disk electrode system. We found that for the cases with pH>7, ORR mainly goes through 4-electron reduction to OH^- at E>pzc (potential of zero charge) without any pH and H-D KIEs. When the pH at the electrode/electrolyte interface (pH^S) is below 7, O_2 only reduces to H_2O_2, its activity increases with pH^S, a H-D KIE of above 2 is observed in 0.1 M $HClO_4$. According to the experiment results in acid solution, a mechanism with $O_2 + H^+ + e \longrightarrow HO_{2,ad}$ as the rate determining step followed by decoupled electron and proton transfer steps is proposed. The high activation barrier for O-O bond breaking and the fast oxidation of H_2O_2 or HO_2^- to O_2 render the ORR can only be observed at potentials negative of the equilibrium potential (E_{eq}) of the redox of H_2O_2/O_2 in acidic media or of HO_2^-/O_2 in alkaline environment. The apparent activation energy ($E_{a,app}$) for O_2 reduction to H_2O_2 is ca. 35 $\pm$ 3 kJ/mol and to OH^- is 60 $\pm$ 6 kJ/mol, while the pre-exponential factor (A) for the former is ca. 3-6 orders of magnitude smaller than that of the latter. The lower activity for O_2 reduction to H_2O_2 at Au(100) is attributed to the small pre-exponential factor.

Keywords: oxygen reduction reaction, pH effect, Au(100) electrode, Kinetic isotope effect, temperature effect, potential determining reaction, rate determining step

1. Introduction:

Because of its important role in fuel cells , oxygen reduction reaction (ORR) has been extensively studied by both experimental and theoretical means.[1-7] Huge amount of molecular level information on ORR mechanism as well as factors which affect ORR kinetics have been achieved.[8-10] ORR kinetics has been found to be very sensitive to the structure and the composition of the electrocatalysts and electrolyte solutions (e.g. pH[6, 11] and coexisting anions[12, 13]and cations[14, 15]). Structure-activity relationship have been derived for many systems, volcano plots on ORR activity versus Gibbs adsorption free energy of O intermediates at the catalysts composed of either bulk single metals,[16, 17]or bimetallic alloys [8, 9, 18-20] has been identified. Such information, in turn, has also leads to better fundamental understanding of the principles of electrocatalysis, e.g., potential determining step (pds) and rate determining step (rds) have been proposed and their distinct roles by affecting the reaction in in thermodynamic and kinetic way have been clarified. [21-23] However, despite of such achievements, great discrepancies still remain on ORR mechanism and factors which limit ORR kinetics. Furthermore, the best catalysts still display overpotential of more than 250 mV at the onset for ORR.

Due to its good stability in wide potential regime region as well as its easiness in preparation, single crystalline Au electrode with different surface orientation has been extensively examined as model electrocatalyst to study ORR.[11-13, 24, 25] It is found that ORR on Au electrode in acidic solutions is a very slow process with H_2O_2 as the final product:[11, 13, 24]

$$O_2 + 2H^+ + 2e \rightleftarrows H_2O_2 \quad (1)$$

While in alkaline solution, reaction may go through

$$O_2 + H_2O + 2e \rightleftarrows HO_2^- + OH^- \quad (2)$$

or

$$O_2 + 2H_2O + 4e \rightleftarrows 4OH^- \quad (3)$$

The first electron-transfer step is suggested to be the rds for all faces in both acidic and basic solution as supported by the fact that the Tafel slope is approximately -120 mV/dec,[26, 27] it is still under debate whether proton or H_2O is involved in the rds.[10, 16, 26] Earlier studies on polycrystalline Au (pc-Au) found that there is no pH effect on ORR at Au in acidic[28] and basic electrolyte.[29] In contrast, our recent study display there is a significant pH effect at pc-Au on ORR

in solutions from 1≤ pH ≤13. [30]

The rate of ORR strongly depends on the plane orientation, Au(100) displays higher activity than other low-index planes.[31] Different origins have been suggested for the good ORR activity at Au(100) in alkaline solution. Based on the lacking of pH effect and that Au(100) has highest ORR activity among all single crystalline faces examined, Adzic et. al. has attributed to the high ORR activity at Au(100) when pH[5]>7 to the specific adsorption of OH^-, which facilitates the adsorption of O_2/HO_2^- and splitting of O-O bond.[29] Based on the fact that in SO_4^{2-}-containing solutions where there is no OH^- adsorption, ORR at Au(100) still exhibits very good activity, Feliu et. al. suggest that the good ORR activity at Au(100) is probably due to the strong adsorption of HO_2^- and the change from 4e-reduction to 2e-reduction at potentials negative of the potential of zero charge (pzc) is attributed to suppression of HO_2^- adsorption and its further reduction due to the increase of electrostatic repulsion at Au(100) toward more negative potentials.[12] From the SERS results and DFT calculations, Gewirth et. al. suggest that the four-electron reduction of O_2 on Au(100) in base arises from a disproportionation mechanism which is enhanced on Au(100) relative to the other two low Miller index faces of Au.[32]. Recent studies by Koper et. al. reveal that quite some electrochemical reactions display much higher activity at (100) surface of Au than at other faces, which is probably linked to the unique ability of (100) terraces to adsorb the reactant, intermediate and to perform bond breaking reactions.[23, 33]

In a word, , there are great deviations between the experimental results for ORR on Au, e.g., it is not clear whether there is pH effect on ORR or not, systematic studies are necessary in order to reach a consensus on the understanding of this system. In this paper, we report and discuss results from our systematic studies on ORR at well-defined Au(100) electrode in 0.1 M $HClO_4$, 0.1 M NaOH, 0.5 M $NaClO_4$+x mM $HClO_4$ and 0.5 M $NaClO_4$+ x mM NaOH solutions with 1≤pH≤13 using hanging meniscus rotating disk electrode (HMRDE) method. H_2O and D_2O are used as solvent to follow the H-D kinetic isotope effects (KIEs) in solution with pH=1 and pH=13. The apparent activation energy ($E_{a,app}$) and the pre-exponential factor (A) for ORR under pH=1 and pH=13 have been derived from temperature dependent polarization curves. Mechanistic and kinetic implication on ORR at Au(100) electrode will be discussed based on present results from the pH effect, temperature, H-D KIEs as well as literature reports.

2. Experimental

The electrolyte solutions of 0.5 M $NaClO_4$ + x mM $HClO_4$ (x= 0.04 to 100) , 0.1 M NaOH or 0.5 M $NaClO_4$ + y mM NaOH (y=1.1 to 107) are prepared using ultra-pure water (18.2 MΩ, from Milli Q water system), perchloric acid (70%, Suprapure) or NaOH (99.99%) together with $NaClO_4$ (99.99%), all the chemicals are from Sigma Aldrich. 0.5 M $NaClO_4$ has been used as supporting electrolyte in order to keep the solution resistance not too high. The N_2 and O_2 gases used in this study are with purity of 99.999% from Nanjing Special gas, corp..

The working electrode (WE) is Au (100) single crystal surface with diameter of 2.4 mm. It is prepared from small bead, obtained by melting and subsequent slow crystallization of Au wire (99.99%, 0.8 mm in diameter, Tanaka Noble Metal Corp.). After cooling, the resulting single crystal bead is oriented (to better than 1°), cut and polished according to Clavilier's technique used for Pt.[34-36] Prior to each experiment the single-crystal electrodes were flame-annealed and quenched with ultrapure water. The electrode surface is covered by a deoxygenated water droplet to avoid contacting with impurities during the transfer to the electrochemical cell. A meniscus configuration is maintained between the Au(100) surface and the electrolyte during all the measurements.

A conventional two-compartment, three electrodes glass cell is used for all the experiments. A lager gold wire is used as counter electrode (CE). For solution with pH=1, a reversible hydrogen electrode (RHE) is used as reference electrode (RE), while for studies in other solutions, a Ag/AgCl (with sat. KCl solution) is used as RE. The Ag/AgCl RE is placed in the 2^{nd} compartment which is connected to the main cell body by a valve connecting with PTFE capillary, in order to avoid the contamination of the solution by the Cl^- ions and by traces of dissolved Ag^+ leaked from the RE. The electrode potentials are controlled by a potentiostat (CHI 760E, ShangHai ChenHua). All potentials in the paper are quoted against the standard hydrogen electrode (SHE), except where stated against RHE specifically.

Before each experiment, all solutions are purged with N_2 for at least 20 min and the base CVs are recorded to make sure that the CVs show well-documented features for Au(100) electrodes. Then O_2 is bubbled into the solution for at least 10 min and the polarization curves for ORR are recorded by cyclic voltammetry under hanging meniscus rotating disk electrode

(HMRDE) configuration at various electrode rotation speeds. The electrode rotation speed is controlled by a modulated rotator (Hokuto Denko Ltd.). During all the electrochemical measurements, the atmosphere in the cell above the electrolyte is purged continuously with same gas as used for the electrolyte. The experiments for pH and H-D KIE are carried out at room temperature (ca. 25±2°C). When studying the temperature effect, a thermostatic cell with glass jacket is used. The cell temperature is controlled by flowing through the glass jacket with water from the thermo-bath of desired temperature. RE is held at room temperature. When recording all the i-E curves for ORR, IR compensation has been carried out automatically by the CHI instrument based on positive-feedback principle; the Ohmic resistance of the electrolyte is measured by current interruption method.

3. Results and Discussion

3.1 Oxygen reduction reaction at Au (100) electrode in x mM NaOH + 0.5 M $NaClO_4$ (pH≥11)

Before discussing the pH effect on ORR at Au(100) electrode in alkaline solution, we will first compare the base cyclic voltammograms (CVs) of Au(100) electrodes recorded in 0.5 M $NaClO_4$ solutions with various concentration of NaOH (11≤pH≤13, Fig. 1). From the CV recorded in 0.1 M NaOH(Fig. 1a, line with star), it is seen that there is a broad double layer region from -0.6 V to 0.1 V and it is followed with a small peak at 0.27 V which is characteristic for the reconstruction of Au(100) surface from hexagonal structure to 1x1 structure.[12, 13] Au oxidation occurs with a broad current wave at E above 0.5 V. In the negative-going potential scan, the reduction of Au(100) occurs at ca. 0.55 V, with peak current at ca. 0.35 V, which is followed with a small shoulder at ca. 0.10 V. Most the features in the CV at Au(100) in 0.1 M NaOH is in well agreement with literature reports.[12, 13] With decrease in solution pH, the peaks for the oxidation of Au(100) and the corresponding reduction peaks of Au oxide shifts to positive potentials. If the curves are plotted against RHE, the onset and peak potentials for Au oxidation and Au oxide reduction are approximately overlapped with each other, which is in well agreement with the fact that such processes involve the exchange of the same amount of electrons and protons. This indicates that the kinetics for Au oxidation and Au oxide reduction do not depend on the solution pH in the range of 11≤pH≤13.

Fig. 2 shows three representative sets of polarization curves of oxygen reduction in 0.5 M

$NaClO_4$+ x mM NaOH with pH=11.1, 12.0 and 13.0 recorded in the positive-going potential scan at various electrode rotation speed from 0 to 2500 rpm. For comparison, the j–E curve recorded at 1500 rpm in the negative-going potential scan in solution is also given. From Fig.2b, it is seen that in solution with pH=12, ORR current increases slightly from -0.45 V to -0.25 V, and it decreases from -0.25 V to -0.05 V, which is followed by a monotonically increase from -0.05 V to 0.28 V. At E above 0.28 V, the current is nearly zero. Except very small shift in the potential (<5 mV), the j-E curves recorded in the negative-going potential scan is nearly the same as that in the positive-going potential scan. The j-E curves recorded in solutions with other pH are quite similar to what with pH=12, except that i) the j-E slope in the potential region form 0.0 V to 0.4 V with pH=11.1 is slightly smaller than that for the cases with higher pH, this is probably a result from the shift of thermodynamic equilibrium potential due to the change of pH at the electrode/electrolyte interface (denoted as pH^s hereafter) during ORR;[5, 37] and ii) the E axis of j-E curves shifts positive with the decrease in solution pH, this is seen clearly from Fig.3a where j-E curves recorded at 2500 rpm in solutions with 11.1≤pH≤13.0 are plotted. It is found that except the j-E curve recorded in solution with pH=11.1, other j-E curves are roughly parallel, the onset potential for ORR and the potential at the half-maximum of ORR current shifts ca. 59 mV/pH(inset in Fig.3). The j-E curves for ORR at Au(100) in all alkaline solutions examined(11≤pH≤13) are found to be qualitatively similar to previous results under similar condition,[11-13] and there is no pH effect on ORR kinetics in solutions with 11≤pH≤13. **The quantitative difference will be discussed below.**

For comparison, the j-E curve for ORR at Pt(111) in 0.1 M NaOH is also included in Fig.2c. From Fig. 2c, it is seen that in the potential region from 0.1 V to 0.2 V, the j-E curves for ORR at Au(100) are very close to that at Pt(111) electrode , revealing that in solutions with pH=13 the ORR activity in the kinetic controlled region is nearly the same at both electrodes. In contrast, at E<0.1 V (i.e., at the potential when current is near half of the maximum ORR current) ORR current density at Pt(111) is significantly higher than that at Au(100), e.g., at -0.1 V, ratio for the current density at these two electrodes are ca. 1.5. It is noticed that the ORR current density at Au(100) in 0.1 M NaOH +0.5 M $NaClO_4$ observed in this study is ca. 30% smaller than what is reported in 0.1 M NaOH reported in the literature.[4, 11, 24] This is probably due to the addition of

$NaClO_4$. Similar phenomenon is also observed in our previous study on pH effect at Pt(111).[5] We have repeated the experiments carefully, and we found that the effect due to the deviation in the height of meniscus shape electrolyte layer under the working electrode is within 5%. This issue has been discussed in detail in our previous paper.[5] Most probable reason for this phenomenon is that O_2 solubility is slightly smaller, while the viscosity ishigher in 0.5 M $NaClO_4$+0.1 M NaOH solutions than that without 0.5 M $NaClO_4$.

No matter in 0.1 M NaOH+0.5 M $NaClO_4$ or just in 0.1 M NaOH, ORR current density at Au(100) at E<0.1 V is smaller than that for ORR at Pt(111) under otherwise identical condition(see Fig. 2c and Fig. 10). If one compare the ORR current in alkaline solutions with other pH, similar phenomenon also exists. This indicates that at Au(100) HO_2^- is produced under these conditions, in contrast to the complete 4e-ORR at Pt(111). This is in contrast to previous conclusion deduced from studies using rotating ring-disk electrode(RRDE), it is claimed that at E>0 V in 0.1 M NaOH O_2 is mainly reduced through 4-electron reaction to OH^- on Au(100) electrode surface, only at E<0 V, incomplete reduction to HO_2^- occurs. [11, 24] The potential of zero charge (E_{pzc}) of unreconstructed Au(100) was found to be 70 mV.[38-40] The onset potential for the 2e-ORR pathway is just close to this E_{pzc} value. We think, the potential-induced changes of the current efficiencies for different ORR pathways may be linked to the potential induced change in the adsorption strength of ORR intermediate, this will be discussed in detail in section 3.3.

3.2 Oxygen reduction reaction at Au (100) electrode in x mM $HClO_4$ + 0.5 M $NaClO_4$ (1≤pH≤4.4)

From the CV recorded in 0.1 M $HClO_4$ (Fig. 4a, line with square), it is seen that there is a broad double layer region from 0 to 1.0 V. And at E above 1.0 V, the current wave are attributed to Au(100) oxidation, as similar to that in alkaline solution. In the negative-going potential scan, the reduction of Au(100) occurs at ca. 1.25 V, with peak current at ca. 1.05 V, with a long tail from 1.0 V to ca. 0.8 V, all the feature for the CV at Au(100) in 0.1 M $HClO_4$ are in well agreement with literature reports.[12, 13] With increase in solution pH, the peak for the oxidation of Au(100) and the corresponding reduction peaks shifts to negative potentials as similar to the case in alkaline solutions with various pH. If the curves are plotted against RHE, the onset and peak potentials for Au oxidation and Au oxide reduction are also overlapped with each other, indicating that in acidic electrolyte the kinetics for Au oxidation and Au oxide reduction also do

not depend on the solution pH. When the pH of bulk solution is 3.7 (Fig.4c), it is found that the reduction peak for Au oxide become much broader than that in solutions with lower pH, and the current wave splits into three separate peaks when the pH of bulk solution is above 3.7. This is caused by the fact that due to the low buffer capability of the bulk solution with medium pH, under stationary condition the pH at the interface changes abruptly during the reduction of Au oxide since proton is fast consumed. As a result some Au oxide has to be reduced at lower potentials where pH^s is above 7, this is similar to our previous observation on the reduction of Pt oxide in un-buffered solutions with medium pH.[37]

Fig. 5 shows three representative sets of polarization curves of oxygen reduction 0.5 M $NaClO_4$+ x mM $HClO_4$ with pH=1.0, 3.0 and 3.7 recorded at various electrode rotation speed from 0 to 1500 rpm. Figs.6 and 7 give the comparison of the j-E curves recorded at 500 rpm in solutions with $1.0 \leq pH \leq 3.0$ and $3.0 \leq pH \leq 4.4$, respectively. In solution with 0.1 M $HClO_4$+0.5 M $NaClO_4$ (Fig.5a), ORR occurs at potentials negative of 0.6 V. The current increases with negative shift in electrode potential, no diffusion-limiting current (j_L) is reached until -0.3 V as similar to what reported previously.[2] With increase in the electrode rotation speed, the ORR current increases, anyway, the current in the mixed control region was lower than $0.5j_L$ of the 4-electron reaction from O_2 to H_2O, this is seen clearly in Fig. 6 where the comparison of the j-E curves for ORR at Au(100) with that at Pt(111) is given. This confirms the preferential reduction of oxygen at Au(100) to hydrogen peroxide.[16, 31, 41] This is further confirmed by the fact that when the electrode is under stationary condition, an anodic current peak due to the oxidation of H_2O_2 appears at ca. 0.7 V (Fig. 5a). H_2O_2 is produced and accumulated near the electrode surface during O_2 reduction at lower potentials.[41] With the increase in the electrode rotation speed to above 200 rpm, no anodic current peak for H_2O_2 oxidation is observed anymore since the H_2O_2 produced diffuse fast away from the electrode surface.

In solution with pH=3, under stationary condition ORR only occurs at E<0.35 V (Fig.5b), and no anodic current peak due to oxidation of H_2O_2 is observed in the potential region up to 0.8 V. With increase in electrode rotation speed, ORR current is found to appear at E<0.6 V, it increases with negative shift in electrode potential and reaches a plateau at around 0.4 V. The current increases again with further negative shift in electrode potential from 0.35 V down to 0.05 V. From 0.05 V to -0.1 V, the current density decreases, and at E<-0.1 V, the current increases again.

The j-E curves recorded in solution with pH=3.7 (Fig.5c) is qualitatively similar to what observed in solution with pH=3, except that current density plateau in the potential region around 0.4 V becomes broader and its magnitude is smaller than that at pH=3 (Fig.5b).

From systematic comparison of the j-E curves recorded in solutions with various pH from 3.0 to 4.4. It is found that the staircase shape of the ORR current wave only appears when the flux of H_3O^+ toward the electrode surface is smaller than two times that of O_2, i.e., $D_{H^+} \cdot c^{b}_{H^+} / \delta_{H^+} < 2 \cdot D_{O_2} \cdot c^{b}_{O_2} / \delta_{O_2}$, where D, c^b and δ are the diffusion coefficients, the concentrations in bulk solution, and the diffusion layer thickness of the corresponding species given in the subscript.[5] The magnitude of the current in the plateau region is proportional to the concentration of proton in the bulk solution (inset in Fig. 7), from the slope it is deduced that two electrons are transferred. This indicates the O_2 is reduced via reduction of O_2 to H_2O_2 in the current plateau region as well as at potentials positive of this current plateau region.

Furthermore, it is found that the lower the solution pH, the more negative the onset potential for the appearance of j_L for O_2 to H_2O_2. This is easily explained by the negative shift in equilibrium potential due to the decrease in the concentration of $[H^+]$. At potential positive of the plateau region, at the same potential versus SHE, the current density for O_2 reduction to H_2O_2 does not show obvious change with solution pH from 3 to 4.4. On the other hand, for the cases with $1 \leq pH \leq 3$, at the same potential versus SHE a clear increase in ORR current with solution pH is noticed. When the j-E curves for O_2 reduction to H_2O_2 for the cases with $1 \leq pH \leq 4.4$ are plotted against RHE (Fig.8b), it is obvious that the overpotential for O_2 reduction to H_2O_2 decreases with increase in pH from 1 to 4.4. This phenomenon is in well agreement with the observation for ORR at pc-Au(Fig.8a),[30] however, it is at various with the case for O_2 reduction to OH^- at Au(100) in alkaline solution (Fig.3, 8b), where no pH dependence is observed.

To have first look, one may think that the increase in the kinetics for O_2 reduction to H_2O_2 for the cases with $1 \leq pH^s \leq 7$ may be due to the fact that when the proton transport is not enough, some O_2 approaching the surface may be reduced through reaction (3). This possibility is excluded since before the set in of the 4-electron reduction processes the diffusion limiting current for O_2 reduction to H_2O_2 is observed (Fig. 7), i.e., the former appears at 0.1 to 0.3 V more negative than the onset j_L for O_2 to H_2O_2.This confirms that when the potential is in the proton

diffusion limiting current region or above, the pH^s is equal or below 7, O_2 reduction to OH^- will not happen. Furthermore, as clearly seen from Fig. 3, the O_2 reduction to OH^- does not change with solution pH in alkaline solution with $11 \leq pH \leq 13$, this is also in contrast to the pH dependence of O_2 reduction to H_2O_2 in acidic environment. Based on these reasons, it is clear that the pH dependence for O_2 reduction to H_2O_2 cannot be attributed to the set in of 4e reduction of O_2 to OH^-, which is superimposed on O_2 reduction to H_2O_2. The origin for the increase in ORR activity at Au(100) with solution pH in the range of $1<pH<7$ will be discussed in detail in section 3.2.

At E<0.3 V in solution with $3.0 \leq pH \leq 4.4$, The j-E curves for ORR increases with further negative shift in electrode potential, this is attributed to 4-electron reduction of O_2 to OH^- which is superimposed on the current wave for O_2 reduction to H_2O_2 which is limited by proton diffusion. The additional current wave for the reduction of O_2 to OH^- is quite similar to what observed in alkaline solution. In the current plateau region, since proton transported to the electrode surface has been completely consumed by reduction of O_2 to H_2O_2, the pH^s at the interface is around 7. The 4-electron reduction of O_2 to OH^- does not immediately occur once reduction of O_2 to H_2O_2 reaches diffusion limiting current for proton. Instead it only occurs at E<0.35 V, this is a result from both the negative shift of the E_{eq} for reduction of O_2 to OH^- with pH^s and the existence of an activation overpotential (of ca. 0.25 V) for this process.[5] In solution with $3.0 \leq pH \leq 4.4$, the onset potential for the reduction of O_2 to OH^- does not show obvious shifts with solution pH, this is due to the fact that in the diffusion limiting potential region for j_L for O_2 to H_2O_2, the pH^s at the interface is around 7 no matter what the pH of the bulk solution is. Once a small amount of O_2 is reduced to OH^-, the pH^s immediately increases to ca. 11, which also does change with the pH of bulk solution.[1, 8]

3.3 Mechanitic and Kinetic implication of ORR at Au(100)

3.3.1 pH and H-D KIE on ORR at Au(100) in alkaline solution The Tafel slope for ORR at Au(100) electrode in alkaline solution is found to be ca. 110-128 mV/dec from the j_k-E plot (inset in Fig.3), where j_k has been derived from the j-E curve recorded at 1500 rpm using the Koutecky-Levich equation and the j_L for ORR at Pt(111) under otherwise identical condition (Fig.2c). This suggests the transfer of first electron is probably the rds for the 4-electron reduction of O_2 to OH^-. On the other hand, from the study of ORR at Au(100) in 0.1 M NaOH with

H_2O and D_2O as solvent (Fig. 9), we found there is barely no KIE for O_2 reduction to OH^- or OD^-. Furthermore, recent SERS studies reveal that $O_2^-{}_{(ads)}$ is detected during ORR at Au electrode in 0.1 M NaOH solution.[32] All the above facts support that the rds for ORR at Au(100) electrode in alkaline medium is probably: [10, 13, 32]

$$O_2 + e \longrightarrow O_2^-{}_{(ads)} \quad (4)$$

However, this contradicts with the view based on thermodynamic consideration, i.e., the lacking of pH effect (on the RHE scale) for ORR (e.g., at Au(100) see Fig.3) should indicate that proton and electron are coupled in the rds, since proton and electron are transferred in the RHE electrode.. Similar problems have also been met from our systematic study on ORR at Pt(111), where in the whole pH range, there is no pH effect on the RHE scale,[5] while both the theoreticians[8, 9, 23, 42] and experimentalists[43-46] suggest that proton and electron transfer are coupled in the rds for ORR at Pt(111). Further studies are necessary to clarify this.

From the base CV, the charge passed during OH^- chemisorption is found to be 120 μC cm^{-2} for Au(100),[24] at the onset potential of ORR its charge decreases toward negative potentials. This trend is just opposite to the increase of ORR current toward more negative potentials. And the DFT calculations show no effect of OH addition to the Au(100) surface with regard to O-O length.[32] Based on the above facts, we think the proposal that the specific adsorption of OH^- facilitates the adsorption of O_2/HO_2^- and the splitting of O-O bond should not be the origin for the high activity for ORR at Au(100) comparing to other crystalline faces. Although present results does not allow us to deduce a detailed mechanism for the 4e-ORR at Au(100) in alkaline media, but very useful information on ORR kinetics can still be deduced (this will be discussed below). From the polarization curve given in Fig.2c, it is seen that at potentials negative of the half wave potential ORR current density at Au(100) is significantly smaller comparing to that at Pt(111) under otherwise identical condition. RRDE experiments also confirm that HO_2^- is produced at Au(100) in alkaline solution.[47] Furthermore, the adsorption of HO_2^- at Au(100) is confirmed by ATR-SEIRAS spectroscopic means under ORR condition.[48] Based on these facts, we agree with the suggestion proposed by Feliu and Koper et al, i.e., the high activity for ORR at Au(100) is probably due its unique ability to adsorb the reactant (O_2), intermediate (HO_2^-) and to perform bond breaking reactions.[12, 33] The conversion from $4e^-$ reduction to $2e^-$ reduction at $E<E_{pzc}$ can also be

easily understood by the suppression of HO_2^- adsorption and its further reduction due to the increase of electrostatic repulsion at Au(100) toward more negative potentials.[12]

Another important question remains to be answered is what determines the onset potential for the 4e-ORR at Au(100) in alkaline environment, which does not depend on the pH of the solution on the RHE scale? The slow kinetics of reaction (4) has been long thought to be the origin for the large activation overpotential at the onset for ORR.[1] If at the same potential versus RHE, the adsorption strength for O_2 and O_2^- intermediate does not change with solution pH, one should expect that the thermodynamic overpotential for ORR, i. e., the difference between E_{eq} for reaction (4) and reaction (3) should decrease with increase in solution pH (the difference between line 4′ and line 3 in Fig. 12), this is opposite to the present experimental observation (Fig.8). This suggests that i) the Gibbs free energy change of reaction (4) has been reduced significantly since the binding strength of O_2^- at Au(100) may be quite high, i.e., the E_{eq} for reaction (4) is closer to the E_{eq} for reaction (3) (it up shifts to the line 4′ in Fig. 12);[32] and ii) there is another process whose thermodynamic overpotential is more unfavorable than that for reaction (4).

"The other process" which is responsible for the onset overpotential for 4e-ORR is probably linked to the key intermediate, i.e., HO_2^-. A few studies on the redox of HO_2^- at Au(100) reveal that the kinetics for both the oxidation and reduction of HO_2^- is very fast.[4, 41] Under ORR condition, despite the further reduction of HO_2^- through reaction (2), its reverse reaction may also take place if the applied potential is not negative enough or the surface concentration of HO_2^- produced is high enough. The dependence of the E_{eq} for reaction (2) as a function of solution pH is plotted in Fig. 12, by taking the surface concentration of HO_2^- is 1 mM (close to the bulk concentration of O_2). Once HO_2^- concentration reaches 1 mM or above, if the applied potential is close to the E_{eq} for reaction (2), it is expected that net ORR current will be nearly zero since both the forward and backward reaction rate may equal. Based on the above analysis, we conclude that reaction (2) is the potential determining reaction (pdr) for the 4e reduction of ORR at Au(100), which determines the onset potential for reaction (3)(Fig.12), i.e.,

$$E^{eq}_{O_2/HO_2^-} = E^0_{O_2/HO_2^-} + \frac{RT}{2F}\ln\frac{a_{O_2}}{a_{HO_2^-}\cdot a_{OH^-}} \quad (5)$$

The lacking of pH dependence of the onset potential for ORR is probably due to the

compensation of counteracting effect of the pH induced shift of E_{eq} of reaction (3) and the pH induced shift of equilibrium concentration of HO_2^- (It should be noticed that this effect is not described in Fig. 12).

In summary, for the 4e ORR at Au(100) in alkaline environment, the rds and pdr are not the same. The pdr determines the upper potential limits where ORR occurs, while the rds determines the rate at the potentials where ORR can occur. Finally, it should be mentioned that at pc-Au electrode (Fig. 8a), a significant pH effect on ORR in alkaline solution is observed.[30] And we found that both the pH independence for ORR at Au(100) and the pH dependence at pc-Au in alkaline solutions are well reproducible. This is probably due to the fact that the surface of pc-Au composed of other faces such as (111) and (110) whose activity are much smaller than that at Au(100), even for Au(100) prepared by different groups or under different experimental conditions the amount of (100) terrace may also be different since it can easily reconstructed to hexagonal configuration. As a result, even in alkaline environment, a significant amount of HO_2^- is produced at such surfaces.[11, 12] Since the amount of HO_2^- at different terraces is different, hence a significant pH effect appears.

3.3.2 ORR in acidic environment The significant smaller current density for ORR at Au(100) in acidic electrolyte (comparing to that at Pt(111), Fig. 6), as well as the corresponding RRDE experiments[16] reveal that the major product under for ORR under such condition is H_2O_2 (Eq. 1). From the comparison of ORR and the redox of H_2O_2 reactions at Au(100) in 0.1 M $HClO_4$ we found that the apparent high overpotential for oxygen reaction at Au(100) is due to i) the extremely weak binding of O_2 and OOH on Au, which renders the breaking of the O-O bond very difficult even after the addition of two protons;[10, 49] and ii) the fast kinetics of H_2O_2 oxidation which limits O_2 reduction to H_2O_2 only occurs at $E < E^{eq}_{O_2/H_2O_2}$:[41]

$$E^{eq}_{O_2/H_2O_2} = E^{0}_{O_2/H_2O_2} + \frac{RT}{2F}\ln\frac{a_{H^+}{}^2 \cdot a_{O_2}}{a_{H_2O_2}} \qquad (6)$$

As similar to that in alkaline solution as discussed above. This is also supported by DFT calculation which reveals that at Au(111) the activation energy (E_a) for hydrogenation of O_2 and OOH is small (0.1 to 0.2 eV), that for O-OH bond breaking is 0.51 eV.[49] Recent DFT calculation demonstrated

that such trend also applies for the case at Au(100) although the absolute values of E_a differs.[10, 11]

From the Tafel plots on the dependence of the kinetic current density on the potential for O_2 reduction to H_2O_2 in the acidic medium (inset in Fig. 6), it is seen that the Tafel slope is close to 120 mV/dec. [41] Furthermore, from ORR at Au(100) in 0.1 M $HClO_4$/$DClO_4$ with H_2O and D_2O as solvents, we found that O_2 reduction to H_2O_2 or D_2O_2 on Au(100) in acidic electrolyte exhibits a H-D kinetic isotope effect (KIE) of above 2 (where KIE=$j_k(E)_{H2O}$/ $j_k(E)_{D2O}$, Fig. 9), indicating that one H^+ or D^+ and one electron is involved in the rds.[41] Based on these two facts, the rds for O_2 reduction to H_2O_2 should be:

$$\mathrm{O_2 + H^+ + e \longrightarrow HO_2} \qquad (5)$$

Possible mechanisms for this reaction are：

Mechanism 1:
$$\begin{aligned} O_2 + H^+ + e^- &\underset{k_{-1}}{\overset{k_1}{\rightleftharpoons}} HO_2 \\ HO_2 + H^+ + e^- &\underset{k_{-2}}{\overset{k_2}{\rightleftharpoons}} H_2O_2 \end{aligned} \qquad (6)$$

Mechanism 2:
$$\begin{aligned} O_2 + H^+ + e^- &\underset{k_{-1}}{\overset{k_1}{\rightleftharpoons}} HO_2 \\ HO_2 + H^+ &\underset{k_{-2}}{\overset{k_2}{\rightleftharpoons}} H_2O_2^+ \\ H_2O_2^+ + e^- &\underset{k_{-3}}{\overset{k_3}{\rightleftharpoons}} H_2O_2 \end{aligned} \qquad (7)$$

Mechanism 3:
$$\begin{aligned} O_2 + H^+ + e^- &\underset{k_{-1}}{\overset{k_1}{\rightleftharpoons}} HO_2 \\ HO_2 + e^- &\underset{k_{-2}}{\overset{k_2}{\rightleftharpoons}} HO_2^- \\ HO_2^- + H^+ &\underset{k_{-3}}{\overset{k_3}{\rightleftharpoons}} H_2O_2 \end{aligned} \qquad (8)$$

Recently, Koper has derived a thermo-electrochemical theory for reactions involving proton and electron transfer.[23] Based on his deduction, the Gibbs free energy changes for the elementary steps of mechanism (1-3) are：

Mechanism (1):
$$\begin{aligned} \Delta G_1 &= G(HO_2) - G(O_2) - G(H^+) + e_0E \\ \Delta G_2 &= G(H_2O_2) - G(HO_2) - G(H^+) + e_0E \end{aligned} \qquad (9)$$

Mechanism (2):
$$\begin{aligned} \Delta G_1 &= -[PA(HO_2) + EA(H_2O_2^+)] + G(H^+) \\ \Delta G_2 &= PA(HO_2) - G(H^+) \\ \Delta G_3 &= EA(H_2O_2^+) \end{aligned} \qquad (10)$$

Mechanism (3):

$$\Delta G_1 = -[EA(HO_2) + PA(HO_2^-] + G(H^+)$$
$$\Delta G_2 = EA(HO_2) \quad (11)$$
$$\Delta G_3 = PA(HO_2^-) - G(H^+)$$

Under equilibrium condition, there is:

$$\Delta G_{total} = 0 \Rightarrow G(H_2O_2) = 2G(H^+) \quad (12)$$

where：

$$G(H^+) = G^\circ(H^+) + RT\ln[H^+] = -2.303RT\square pH \quad (13)$$

The step with highest Gibbs free energy change is defined as the potential determining step (pds), the thermodynamic overpotential is defined as its equilibrium potential of the pds subtracts the equilibrium potential for the overall reaction. From Eqs. (9 to 13), it is derived that the thermodynamic overpotential for mechanism (1) will not depend on solution pH, based on the significant increase in ORR activity with solution pH mechanism (1) can be excluded. On the other hand, the thermodynamic overpotential for mechanism (2) and (3) are

$$\eta_T = \frac{2.303RT(pK_a - pH)}{2F} \quad (14)$$

From Eq. 14, it is seen that if the transfer of one of the electron and proton transfer is decoupled, the optimal catalytic activity (with smallest thermodynamic overpotential) will appear in solution with pH=pK_a. Since the pK_a for H_2O_2 is 11.8.

$$H_2O_2 \rightleftharpoons HO_2^- + H^+ \quad (15)$$

The increase in the activity of reaction (1) with pH up to 7 may be easily explained by it goes through either mechanism (2) or (3).

On the other hand, the E_{pzc} for Au(100)-(1x1) in 0.1 M $HClO_4$ is ca. 0.33 V(SHE), [50] i.e., in the potential region close to the onset for O_2 reduction to H_2O_2, the formation and strong adsorption of $H_2O_2^+$ is less likely due to the electrostatic repulsion. Furthermore, recent infrared spectroscopic studies reveal that $HO_{2,ad}^-$ is detected during ORR at Au film electrode in 0.5 M $HClO_4$ solution.[51] All the above facts support that mechanism (3) is most probable for O_2 reduction to H_2O_2 at Au(100) in acidic environment ($pH^s \leq 7$), provided that only one reaction channel operates and the mechanism for O_2 reduction in electrolyte with $1 \leq pH^s \leq 7$ does not change with solution pH^s.

3.3.3 Temperature effect on ORR at Au(100) In order to understand the difference in the

reaction kinetics of the 2e- and 4e-ORR process and to figure out the possible origin for the slower kinetics for the reduction of O_2 to H_2O_2 on Au(100) than that for the reduction of O_2 to OH^-, we have carried out systematic study on ORR at Au(100) in 0.1 M $HClO_4$ and 0.1 M NaOH at temperatures of 5, 15, 20, 30 and 40°C (Fig. 10). By carefully repeating the experiments, we found that the j-E curves are well reproducible. The values of j_K at different potential is derived from the K-L equation taking half of the diffusion limiting current and the diffusion limiting current for ORR at Pt(111) measured under otherwise identical condition as the j_L for the 2e-ORR process in 0.1 M $HClO_4$ and for the 4e-ORR process 0.1 M NaOH, respectively. Rate constant k(E) at each potential is derived by calibrating the change of O_2 concentration with temperature from[52, 53]

$$j_k = nFkc_{O_2}^b \quad (17)$$

And the apparent activation energy ($E_{a,app}$) and the pre-exponential factor (A) for O_2 reduction reaction in 0.1 M $HClO_4$ and 0.1 M NaOH solution as function of reaction potential are derived from the k(E)~1/T plot. Since in 0.1 M NaOH, ORR will shift from 4e-process to both 4e- and 2e-ORR process at E negative of 0.1 V(Fig. 2c), hence only $E_{a,app}$ at E from the onset potential to 0.1 V for ORR is calculated, it is assumed that in this potential region, only 4e-ORR occurs. We found $E_{a,app}$ for the $2e^-$ and $4e^-$ORR at Au(100) in 0.1 M $HClO_4$ and 0.1 M NaOH solution are ca. 35±3 kJ/mol and ca. 60±2 kJ/mol, respectively (Fig. 10b). The $E_{a,app}$ in acidic electrolyte is ca. 25 kJ/mol smaller than that in alkaline solution. In contrast, the prefactor A at the onset potential for the reaction is 3-6 orders of magnitude times smaller in 0.1 M $HClO_4$ than that for ORR at 0.1 M NaOH solution. The fact , i.e., $E_{a,app}$ and A for ORR at Au(100) in 0.1 M NaOH are significantly higher than those in 0.1 M $HClO_4$, and ORR activity for the former case is higher than for the latter case, implies that the pre-exponential factor is a better descriptor for ORR activity than that for the activation energy.

Furthermore, it is found that in acid solution, $E_{a,app}$ and A first decrease with electrode potential from 0.7 V to 0.4 V, and then both increase with further negative shifts with potential(Fig. 11). The phenomenon that $E_{a,app}$ and A change in the same direction upon the change of a certain experimental parameter are widely observed in gas phase catalysis, which is called as compensation effect. [54] The origin of such phenomenon is still under discussion.[54] It is

proved that simple mechanisms with realistic parameters display such signatures without a change in rate limiting step and in the absence of transport phenomena. We think such a situation may also work for the present case of ORR at Au(100), i.e., ORR mechanism does not change with potential at all. Since 0.33 V is just the pzc for Au(100) in 0.1 M $HClO_4$,[50] the potential dependent change is probably related to the potential-dependent change in adsorption strength of O_2 and HO_2^-.[12]

It is interesting to discuss that at $E<E_{pzc}$, the $E_{a,app}$ for O_2 reduction to H_2O_2 increases with negative shift in electrode potential, this is just opposite to the prediction by Butler-Volmer theory. Under such conditions, the reduction in ORR activity due to the increase in E_a is overcompensated by the increase in the pre-exponential factor, as a result, a net increase in the rate with negative shift in electrode potential is observed. The increase in $E_{a,app}$ toward negative potential may be explained by the decrease in the adsorption strength O_2 and HO_2 intermediate. Temperature effect on ORR at Au(100) has not been examined widely, preliminary study by Markovic et al found that the ORR current at Au(100) in 0.1 M NaOH does not show obvious increase with temperature,[4] hence they have not estimated the $E_{a,app}$ at all. From DFT calculation, Quaino et al. found that with the applied overpotential of 300 mV for oxygen reduction on Au(100) electrode, the activation energy for the outer-sphere reaction of the first electron transfer is about 0.47 eV and the activation energy from the Marcus theory is 0.65 eV,[10] the latter is close to our results in alkaline solution. However，the significant dependence of ORR activity with orientation of Au single crystalline, indicates that this process should take place in a catalytic way rather than as an outer-sphere reaction. The increase in the pre-exponential factor with negative shift in electrode potential implies that there is a positive entropy contribution. Further theoretical studies with are underway to get more molecular level information on such changes.

4. Conclusions

pH, temperature and H-D kinetic isotope effects O_2 reduction at Au(100) has been examined systematically using HMRDE system in a wide pH($1\leq pH\leq 13$) and temperature range(5-40°C). When $pH^s>7$, at E>PZC, O_2 is found to mainly going through 4-electron reduction to OH^- and no pH and H-D KIE effect on ORR activity is observed. Under conditions when the pH^s at the electrode/electrolyte interface is below 7, O_2 is mainly reduced to H_2O_2, whose activity is found

to increases with pH^S. A H-D KIE of above 2 is observed in acidic electrolyte. A Tafel slope of ca. 120 mV/dec has been found both in acid and alkaline solutions. The rds for O_2 reduction to H_2O_2 and OH^- are found to be $O_2 + H^+ + e \longrightarrow HO_{2,ad}$ and $O_2 + e \longrightarrow O_{2,ad}^-$, respectively. The fast electrochemical oxidation of H_2O_2 or HO_2^- to O_2 render the ORR in acidic and alkaline environment can only be observed at potentials negative of the E_{eq} for reaction (1) and (2), respectively.

The increase in ORR activity with pH^S for cases with $pH^S<7$ is well explained by a mechanism with $O_2 + H^+ + e \longrightarrow HO_{2,ad}$ as the rds, which follows with decoupled electron and proton transfer steps. The apparent activation energy ($E_{a,app}$) for O_2 reduction to H_2O_2 (to OH^-) is ca. 35 $\pm$ 3 kJ/mol (60$\pm$6 kJ/mol), while the pre-exponential factor (A) for the former is ca. 3-6 orders of magnitude times smaller than that of the latter. The lower activity for O_2 reduction to H_2O_2 than that for O_2 reduction to OH^- at Au(100) is attributed to its smaller pre-exponential factor, which is linked to an unfavorable entropy effect.

Acknowledgement

This work is supported by National Natural Science Foundation of China (NSFC) (project's no. 21073176), National Instrumentation Program (no. 2011YQ03012416) and 973 Program (no. 2010CB923302) from the ministry of science and technology of China.

References

1. F. J. Vidal-Iglesias, J. Solla-Gullón, E. Herrero and J. M. Feliu, in *Electrocatalysis in Fuel Cells*, Springer, 2013, pp. 483-512.
2. S. Strbac, N. A. Anastasijević and R. R. Adžić, *J. Electroanal. Chem.*, 1992, **323**, 179-195.
3. J. K. Norskov, J. Rossmeisl, A. Logadottir, L. Lindqvist, J. R. Kitchin, T. Bligaard and H. Jonsson, *J. Phys. Chem. B*, 2004, **108**, 17886-17892.
4. T. J. Schmidt, V. Stamenkovic, M. Arenz, N. M. Markovic and P. N. Ross, *Electrochim. Acta*, 2002, **47**, 3765-3776.
5. M. F. Li, L. W. Liao, D. F. Yuan, D. Mei and Y.-X. Chen, *Electrochim. Acta*, 2013, **110**, 780-789.
6. M. Tarasevich and O. Korchagin, *Russ. J. Electrochem.*, 2013, **49**, 600-618.
7. M. Tarasevich, A. Sadkowski and E. Yeager, *Oxygen electrochemistry*, Springer, 1983.
8. V. Viswanathan, H. A. Hansen, J. Rossmeisl and J. K. Norskov, *J. Phys. Chem. Lett.*, 2012, **3**, 2948-2951.
9. V. Viswanathan, H. A. Hansen, J. Rossmeisl and J. K. Norskov, *Acs. Catal.*, 2012, **2**, 1654-1660.
10. P. Quaino, N. B. Luque, R. Nazmutdinov, E. Santos and W. Schmickler, *Angew. Chem., Int. Ed.*, 2012, **51**, 12997-13000.

11. S. Strbac and R. R. Adzic, *Electrochim. Acta*, 1996, **41**, 2903-2908.
12. A. Prieto, J. Hernandez, E. Herrero and J. M. Feliu, *J. Solid State Electrochem.*, 2003, **7**, 599-606.
13. B. B. Blizanac, C. A. Lucas, M. E. Gallagher, M. Arenz, P. N. Ross and N. M. Markovic, *J. Phys. Chem. B*, 2004, **108**, 625-634.
14. D. Strmcnik, K. Kodama, D. van der Vliet, J. Greeley, V. R. Stamenkovic and N. M. Markovic, *Nat. Chem.*, 2009, **1**, 466-472.
15. B. B. Berkes, G. Inzelt, W. Schuhmann and A. S. Bondarenko, *J. Phys. Chem. C*, 2012, **116**, 10995-11003.
16. V. Andoralov, M. Tarasevich and O. Tripachev, *Russ. J. Electrochem.*, 2011, **47**, 1327-1336.
17. A. Appleby, *Catal. Rev.*, 1971, **4**, 221-244.
18. D. Strmcnik, M. Escudero-Escribano, K. Kodama, V. R. Stamenkovic, A. Cuesta and N. M. Markovic, *Nat. Chem.*, 2010, **2**, 880-885.
19. J. Greeley, I. E. L. Stephens, A. S. Bondarenko, T. P. Johansson, H. A. Hansen, T. F. Jaramillo, J. Rossmeisl, I. Chorkendorff and J. K. Norskov, *Nat. Chem.*, 2009, **1**, 552-556.
20. V. Stamenkovic, B. S. Mun, K. J. J. Mayrhofer, P. N. Ross, N. M. Markovic, J. Rossmeisl, J. Greeley and J. K. Norskov, *Angew. Chem., Int. Ed.*, 2006, **45**, 2897-2901.
21. M. T. Koper, *J. Solid State Electrochem.*, 2013, **17**, 339-344.
22. M. T. M. Koper, *J. Electroanal. Chem.*, 2011, **660**, 254-260.
23. M. T. M. Koper, *Chem. Sci.*, 2013, **4**, 2710-2723.
24. S. Strbac and R. R. Adzic, *J. Electroanal. Chem.*, 1996, **403**, 169-181.
25. N. M. Markovic, I. M. Tidswell and P. N. Ross, *Langmuir*, 1994, **10**, 1-4.
26. R. Adzic, *Recent advances in the kinetics of oxygen reduction*, Brookhaven National Lab., Upton, NY (United States), 1996.
27. J. Lipkowski, L. Stolberg, D.-F. Yang, B. Pettinger, S. Mirwald, F. Henglein and D. Kolb, *Electrochim. Acta*, 1994, **39**, 1045-1056.
28. M. Genshaw, A. Damjanovic and J. M. Bockris, *J. Electroanal.Interf. Chem.*, 1967, **15**, 163-172.
29. R. Zurilla, R. Sen and E. B. Yeager, *J. Electrochem. Soc.*, 1978, **125**, 1103.
30. Q. Chen, Y. Zheng, L. Liao, J. Kang and Y. Chen, *Scientia Sinica Chimica*, 2011, **41**, 1777.
31. M. Alvarez-Rizatti and k. Juttner, *J. Electroanal. Chem.*, 1982, **144**, 351-358.
32. J. W. Kim and A. A. Gewirth, *J. Phys. Chem. B*, 2006, **110**, 2565-2571.
33. H. Li, F. Calle-Vallejo, M. J. Kolb, Y. Kwon, Y. Li and M. T. Koper, *J. Am. Chem. Soc.*, 2013, **135**, 14329-14338.
34. J. Clavilier, D. Armand, S. G. Sun and M. Petit, *J. Electroanal. Chem.*, 1986, **205**, 267-277.
35. J. Clavilier, R. Faure, G. Guinet and R. Durand, *J. Electroanal. Chem.*, 1980, **107**, 205-209.
36. J. Clavilier, *J. Electroanal. Chem.*, 1980, **107**, 211-216.
37. L. W. Liao, M. F. Li, J. Kang, D. Chen, Y.-X. Chen and S. Ye, *J. Electroanal. Chem.*, 2013, **688**, 207-215.
38. A. Hamelin, *J. Electroanal. Chem.*, 1995, **386**, 1-10.
39. D. Kolb and J. Schneider, *Electrochim. Acta*, 1986, **31**, 929-936.
40. D. Kolb and J. Schneider, *Surf. Sci.*, 1985, **162**, 764-775.
41. Y. L. Zheng, D. Mei, Y.-X. Chen and S. Ye, *Electrochem. Commun.*, 2014, **39**, 19-21.
42. J. A. Keith and T. Jacob, *Angew. Chem., Int. Ed.*, 2010, **49**, 9521-9525.
43. D. B. Sepa, M. V. Vojnovic and A. Damjanovic, *Electrochim. Acta*, 1981, **26**, 781-793.
44. D. B. Sepa, M. V. Vojnovic, L. M. Vracar and A. Damjanovic, *Electrochim. Acta*, 1987, **32**, 129-134.

45. M. R. Tarasevich, R. K.Burshtein and K. A. Radyushkina., *Elektrokhimiya*, 1970, **6**, 372-375.
46. M. R. Tarasevich, *Elektrokhimiya*, 1973, **9**, 599-605.
47. R. W. Zurilla, R. K. Sen and E. Yeager, *J. Electrochem. Soc.*, 1978, **125**, 1103-1109.
48. M. H. Shao and R. R. Adzic, *J. Phys. Chem. B*, 2005, **109**, 16563-16566.
49. D. C. Ford, A. U. Nilekar, Y. Xu and M. Mavrikakis, *Surf. Sci.*, 2010, **604**, 1565-1575.
50. L. A. Kibler, *Preparation and Characterization of Noble Metal Single Crystal Electrode Surfaces* International Society of Electrochemistry, 2003.
51. N. Ohta, K. Nomura and I. Yagi, *J. Phys. Chem. C*, 2012, **116**, 14390-14400.
52. N. Wakabayashi, M. Takeichi, M. Itagaki, H. Uchida and M. Watanabe, *J. Electroanal. Chem.*, 2005, **574**, 339-346.
53. U. A. Paulus, T. J. Schmidt, H. A. Gasteiger and R. J. Behm, *J. Electroanal. Chem.*, 2001, **495**, 134-145.
54. H. Lynggaard, A. Andreasen, C. Stegelmann and P. Stoltze, *Prog. Surf. Sci.*, 2004, **77**, 71-137.

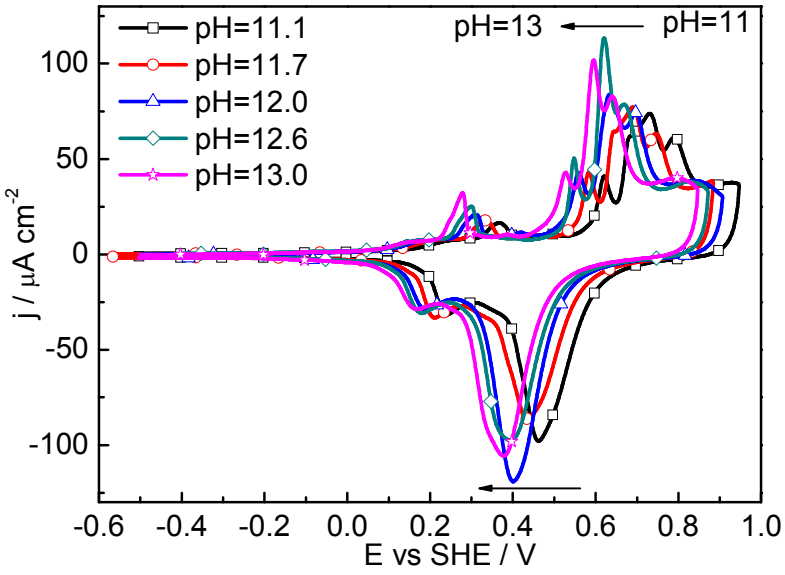

Fig.1 Cyclic voltammograms of Au(100) electrode in N_2 saturated 0.5 M $NaClO_4$ solution with 1.1 mM (square), 4.5 mM (circle), 10 mM (triangle), 36.3 mM (diamond) or 107 mM (star) NaOH, potential scan rate: 50 mV/s.

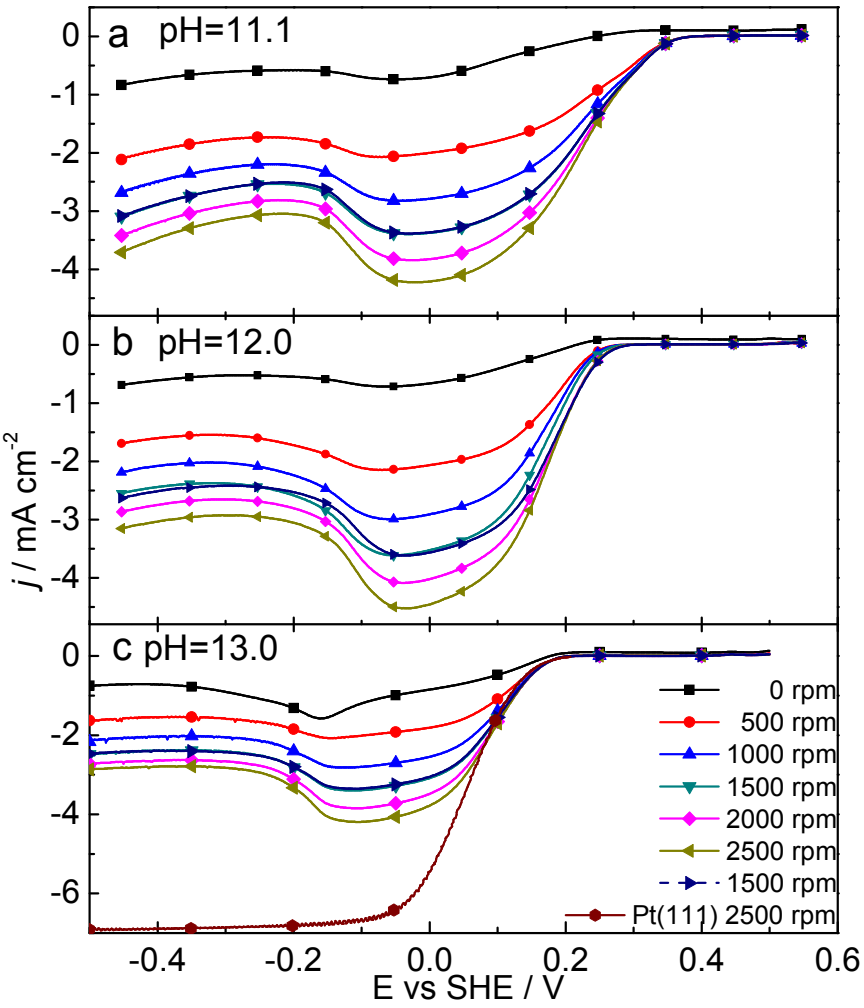

Fig. 2 Positive-going scan polarization curves of ORR at Au (100) electrode in O_2 saturated 0.5 M $NaClO_4$ solution with (a) 1.1 mM, (b) 10 mM NaOH and (c) 100 mM NaOH under various electrode rotation speed from 0 to 2500 rpm, dashed line is the i-E curve recorded in the negative-going potential scan at 1500 rpm, scan rate 50 mV/s. For comparison, i-E curve for ORR at Pt (111) in 0.1 M NaOH+0.5 M $NaClO_4$ (pentagon) at 2500 rpm is also given in panel c.

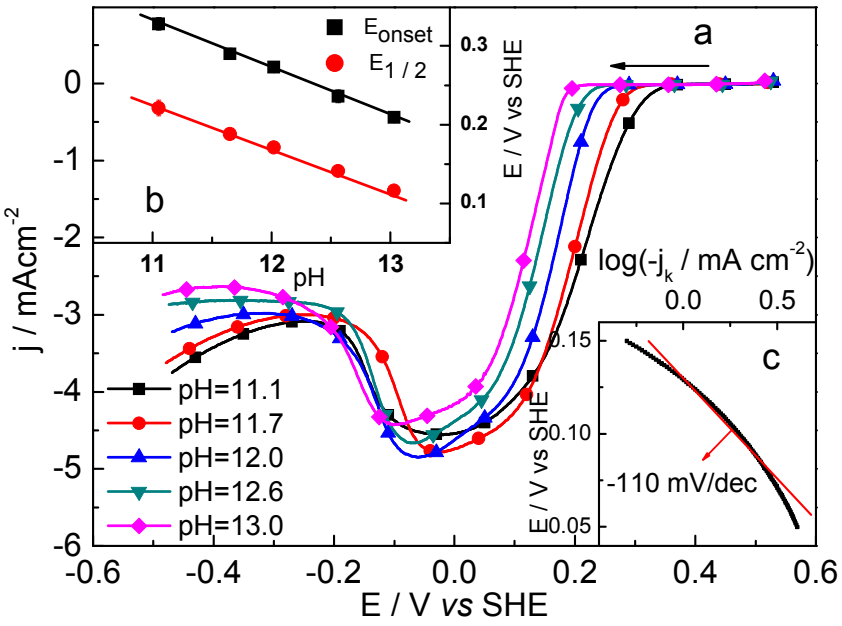

Fig. 3 (a) positive-going polarization curves of ORR at Au (100) electrode in O_2 saturated 0.5 M $NaClO_4$ solution with 1.1 mM (square), 4.5 mM (circle), 10 mM (triangle), 36.3 mM (diamond) or 107 mM (star) NaOH at potential scan rate of 50 mV/s and electrode rotation speed of 2500 rpm. (b) The onset potential (black square) and the potential of half maximum current (red circle) of ORR at Au (100) electrode as a function of solution pH (square and circle dots are the raw data; solid line is the linear fitting for the data points). (c) The corresponding Tafel plots of the j_k-E plot for ORR at Au(100) in 0.1 M NaOH solution, j_k is derived from K-L equation.

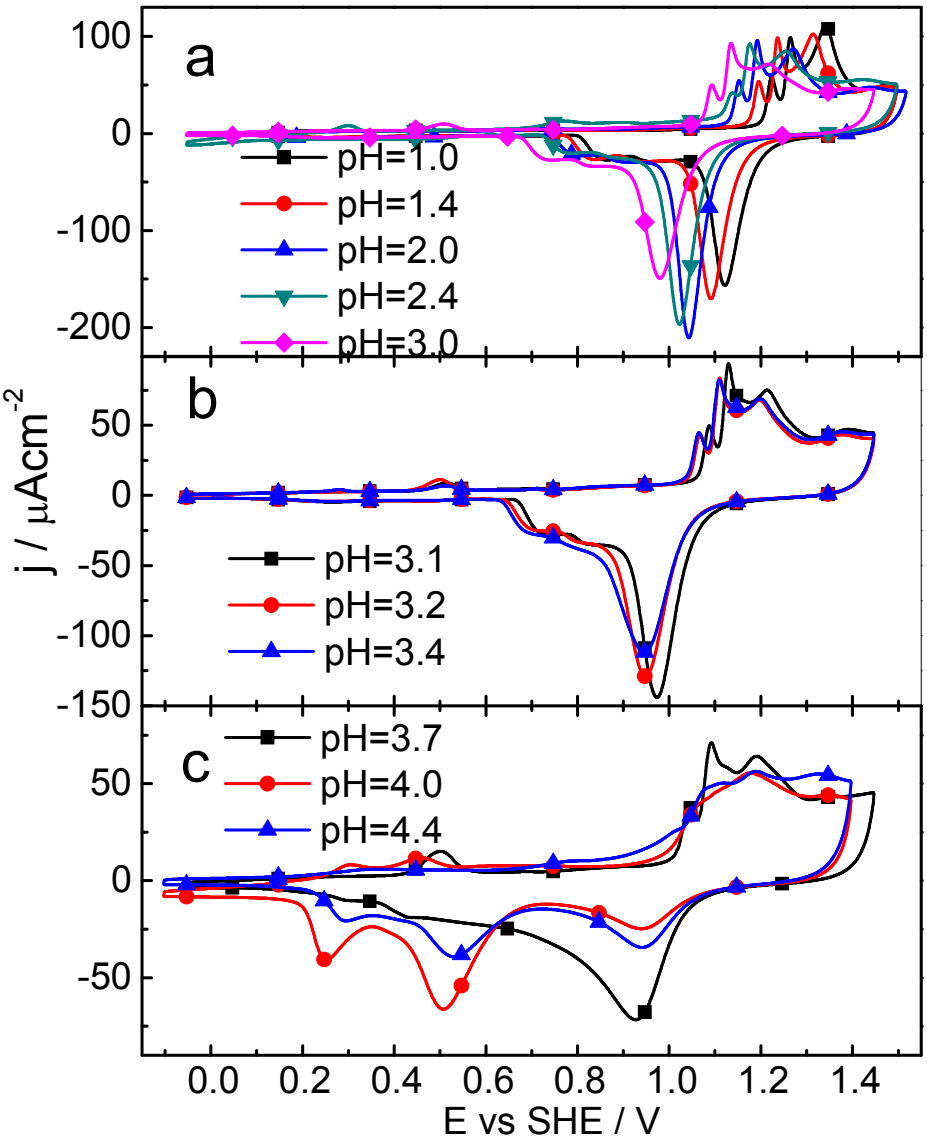

Fig.4 Cyclic voltammograms of Au (100) electrode in N_2 saturated 0.5 M $NaClO_4$ + x mM $HClO_4$ solution with x= (a) 0.1 M (square) , 39 mM (circle), 10 mM (triangle), 3.6 mM (star), 1 mM (diamond) , (b) 0.8 mM (square), 0.6 mM (circle), 0.36 mM (triangle) and (c) 0.2 mM (square), 0.1 mM (circle), 0.04 mM (triangle), potential scan rate: 50 mV/s.

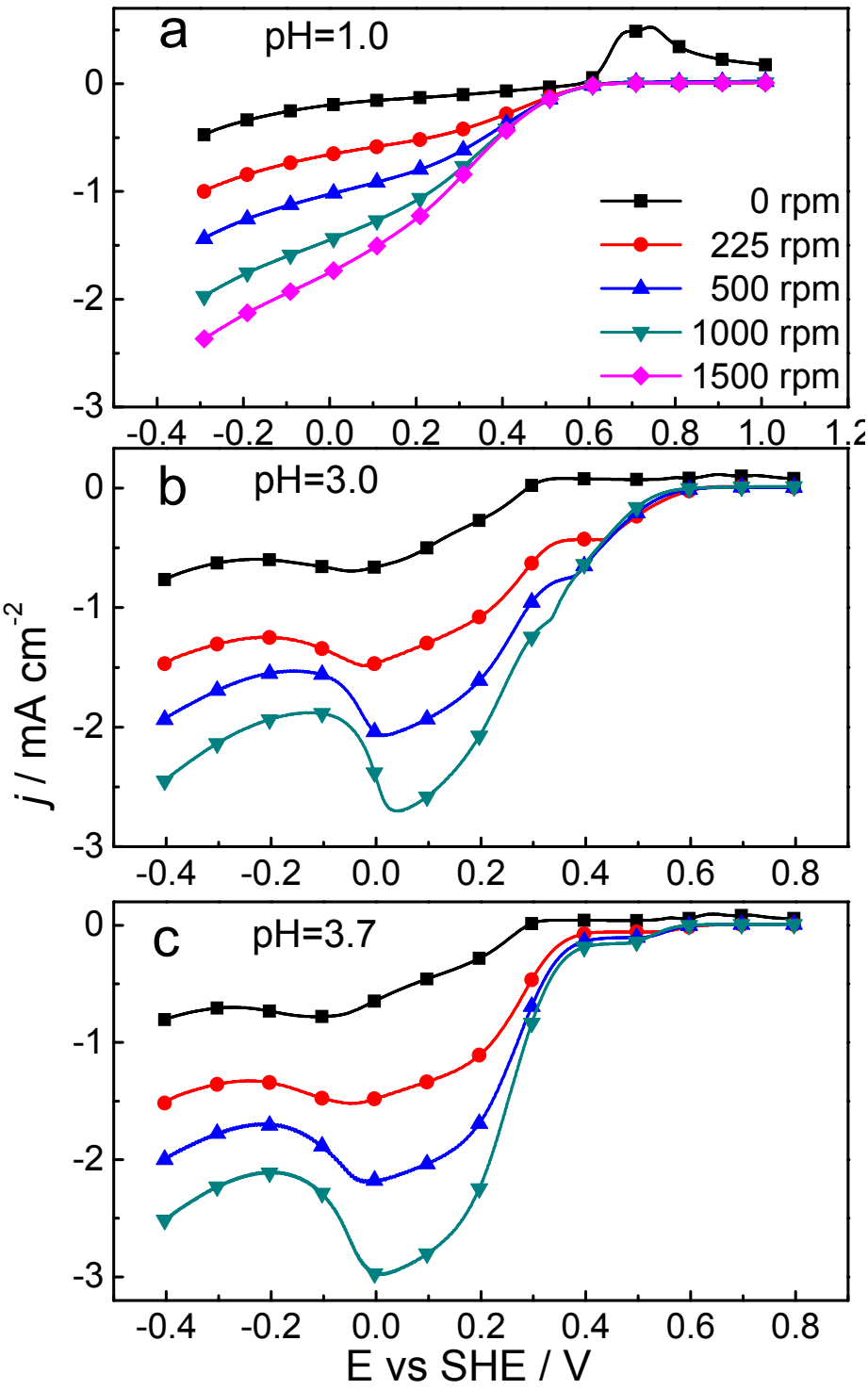

Fig. 5 Positive-going scan polarization curves of ORR at Au (100) electrode in O_2 saturated 0.5 M $NaClO_4$ with (a) 0.1 M, (b) 1 mM or (c) 0.2 mM $HClO_4$ under various electrode rotation speeds from 0 to 1500 rpm, potential scan rate: 50 mV/s.

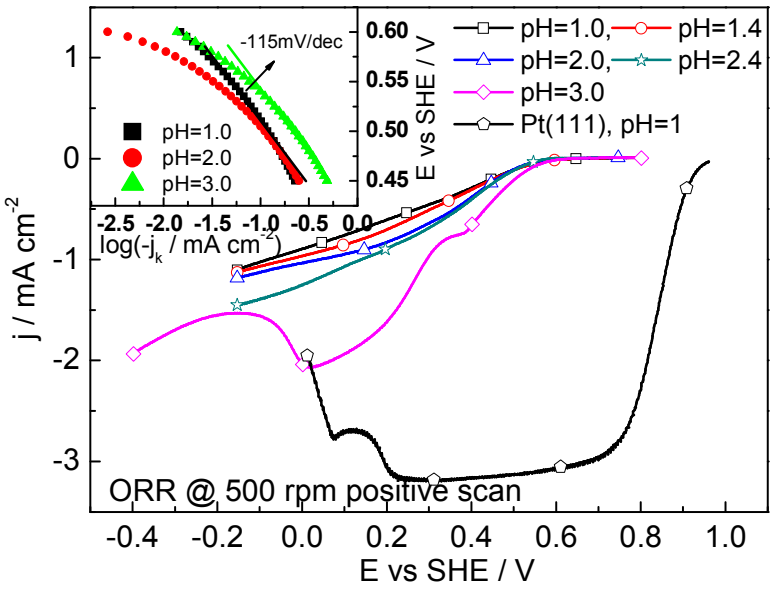

Fig. 6 Positive-going scan polarization curves of ORR at Au (100) electrode in O_2 saturated 0.5 M $NaClO_4$ solutions with 100 mM (square), 39 mM (circle), 10 mM (triangle), 3.6 mM (star) or 1 mM (diamond) $HClO_4$ at potential scan rate of 50 mV/s and electrode rotation speed of 500 rpm. For comparison, i-t curve for ORR at Pt(111) in 0.1 M $HClO_4$ (pentagon) is also given. Inset: The corresponding Tafel plots of the j_k-E plot for ORR at Au(100) for the cases with pH=1, 2 and 3, j_k is derived from K-L equation, the j_L for 2e-ORR at Au(100) is supposed to equal 1/2 j_L for 4e-ORR at Pt(111) under the same electrode rotation speed.

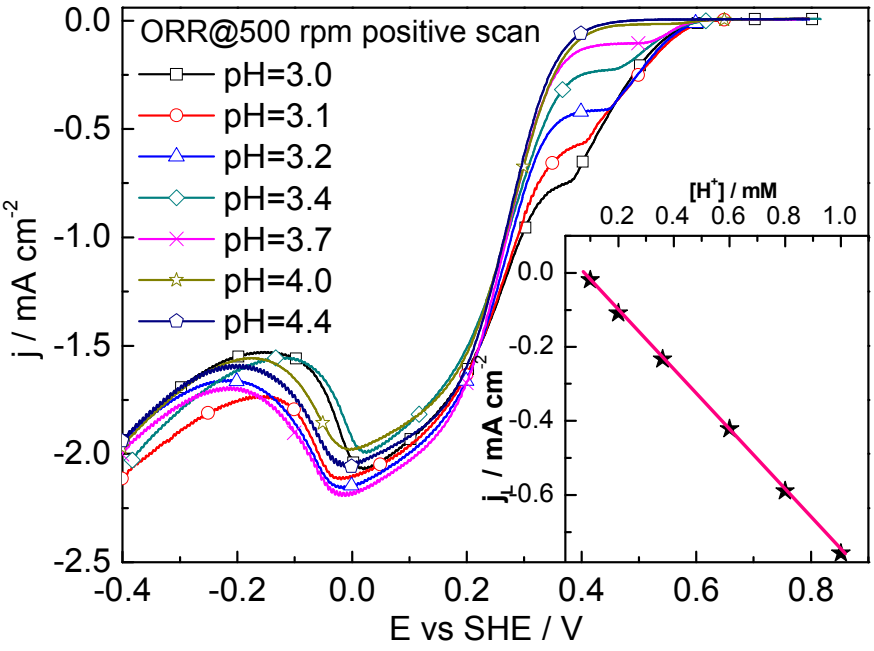

Fig. 7 Positive-going scan polarization curves of ORR at Au (100) electrode in O_2 saturated 0.5 M $NaClO_4$ solution with 1mM (square) , 0.8 mM (circle), 0.6 mM (triangle), 0.36 (diamond), 0.2 mM (cross), 0.1 (star) or 0.04 mM (pentagon) $HClO_4$ at potential scan rate of 50 mV/s and electrode rotation speed of 500 rpm. Inset: plot of the diffusion current density (the current plateau at 0.4 V) for $O_2+4H^++4e^-\rightarrow 2H_2O$ as a function of $[H^+]$ in the bulk solution.

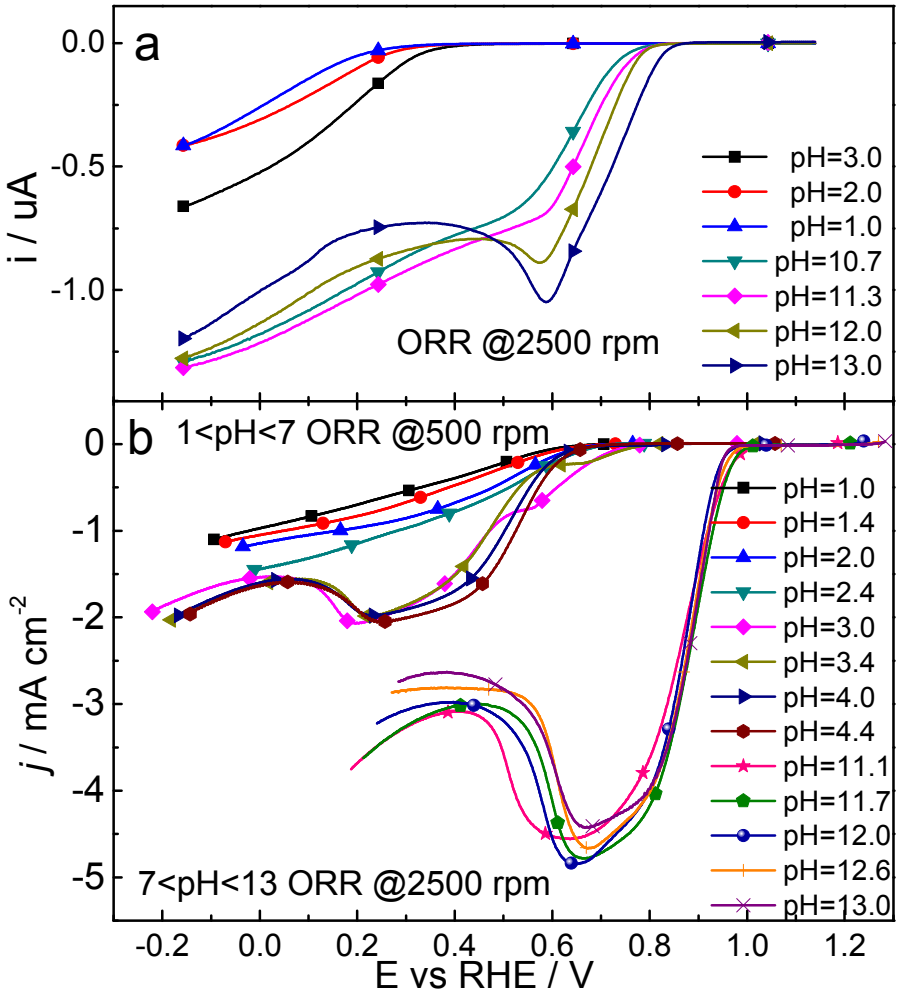

Fig. 8 Polarization curves for ORR as a function of solution pH at a) pc-Au electrode (the data is reproduced from ref. 31 and the electrode rotation speed is 2500 rpm) and b) Au(100) electrode, data from Figs. 6 and 3, but with electrode potential versus RHE. In acid solution the ORR measured at positive-going potential scan and electrode rotation speed is 500 rpm and in alkaline solution the ORR measured at negative-going potential scan and at electrode rotation speed of 2500 rpm .

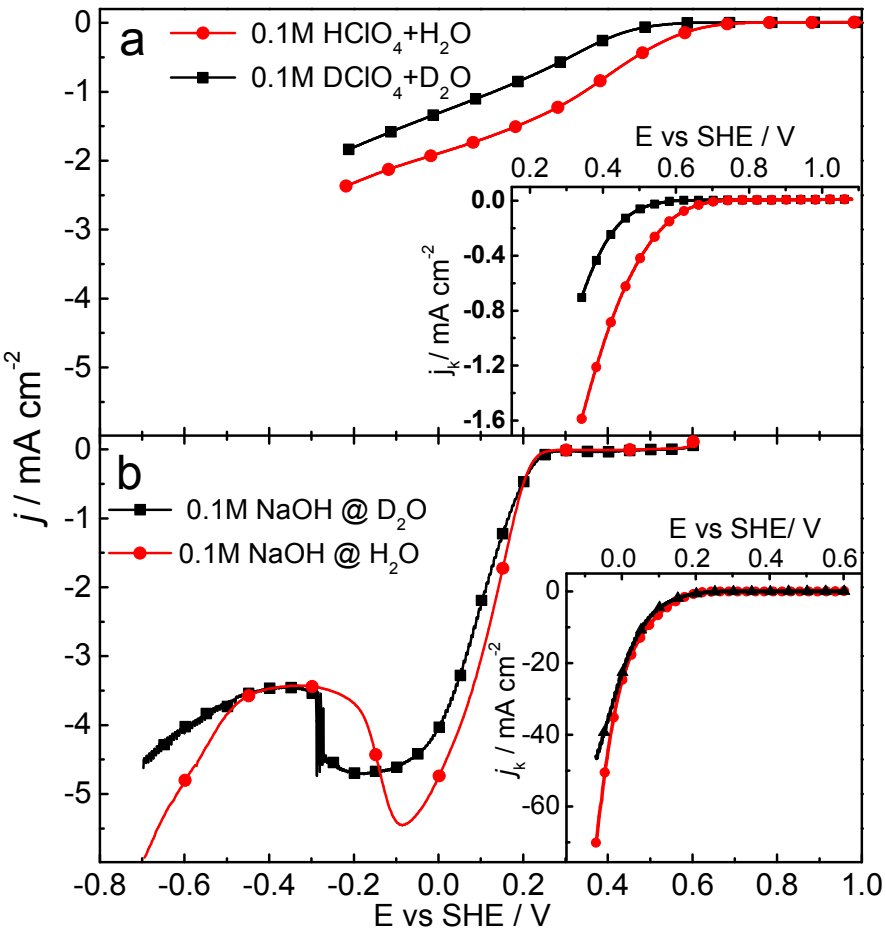

Fig.9 Positive-going polarization curves for O_2 reduction at Au (100) electrode in (a) 0.1 M $HClO_4$+H_2O (circle) and 0.1 M $DClO_4$+D_2O (square) solutions at electrode rotation speed of 1500 rpm, and (b) 0.1 M NaOH+H_2O (circle) and 0.1 M NaOH +D_2O (square) solutions at 2500 rpm. Inset shows the corresponding kinetics current densities as a function of potential. Data in panel a are reproduced from ref. 31.

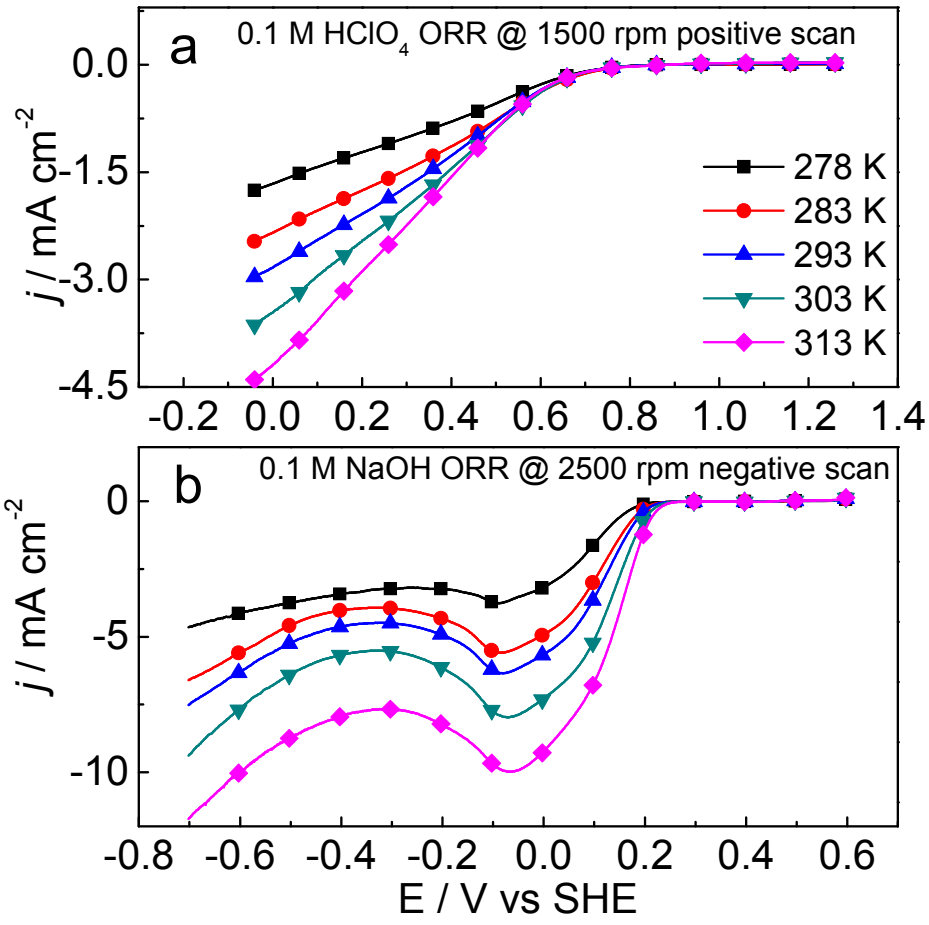

Fig.10 The ORR polarization curves at Au(100) measured at different temperatures in (a) 0.1 M $HClO_4$, (b) 0.1 M NaOH. Scan rate, 50 mV/s.

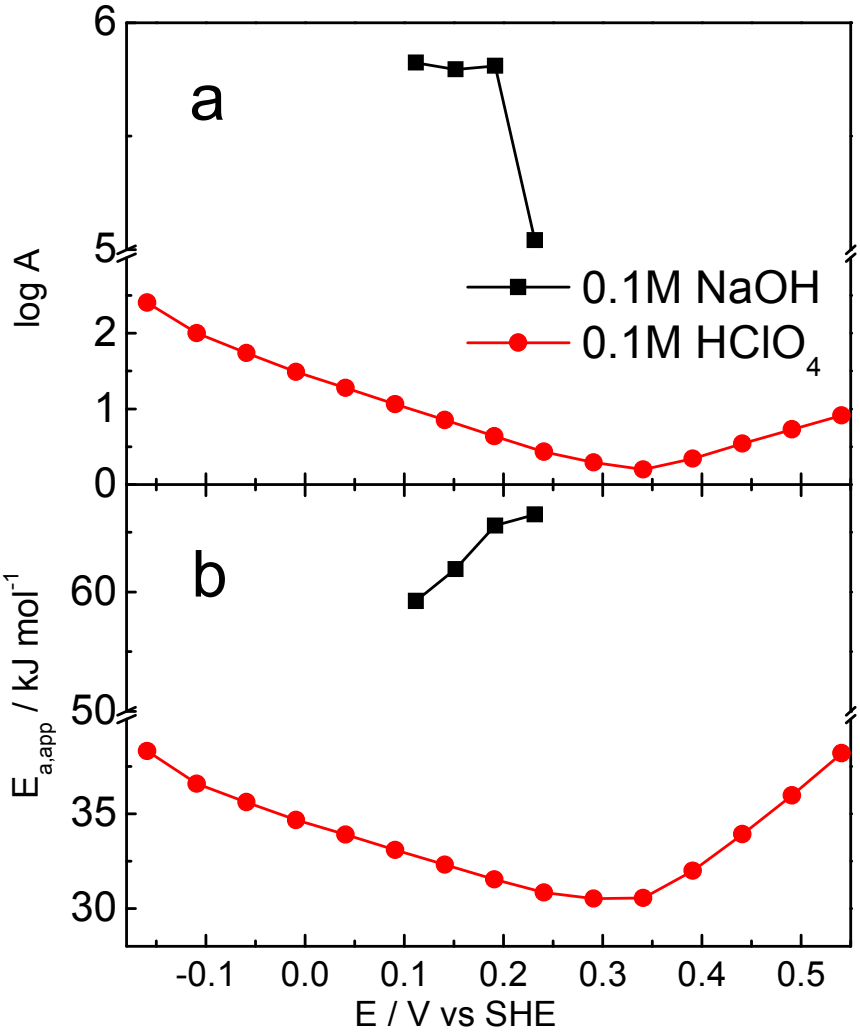

Fig.11 Pre-exponential factor (a) and the apparent activation energy (b) for the O_2 reduction to H_2O_2 and OH^- on Au (100) in 0.1 M $HClO_4$ and 0.1 M NaOH, data is derived from k(E)~1/T plots deduced from ORR polarization curves recorded at 5, 15, 20, 30 and 40°C after the calibration of temperature dependent change in O_2 solubility.

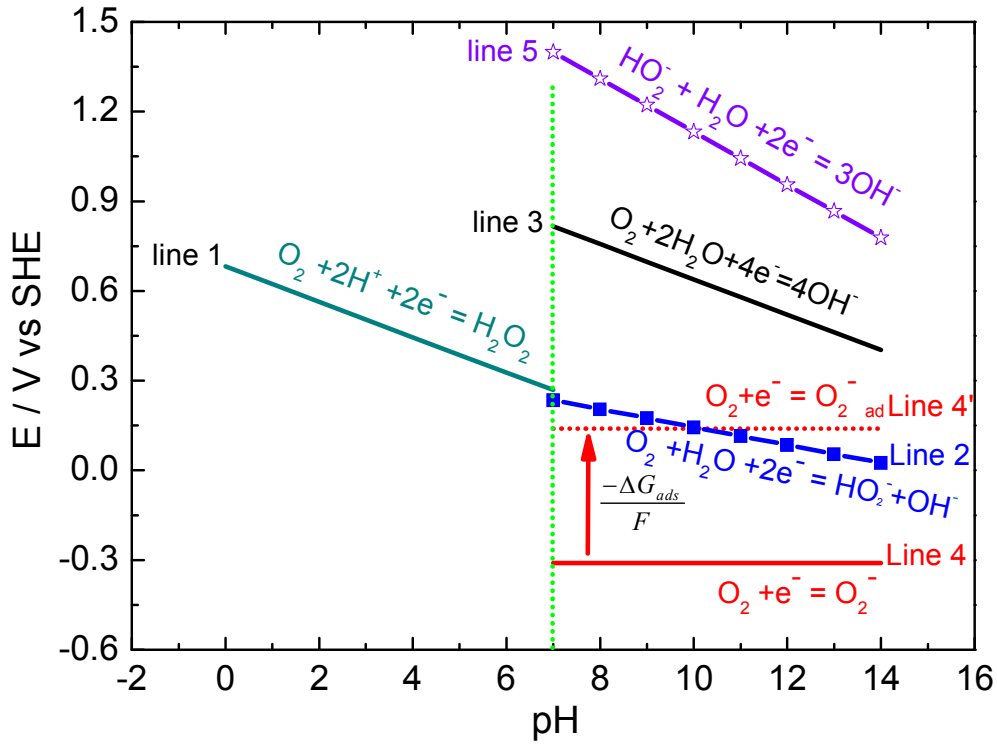

Fig. 12 Pourbaix diagram of possible reactions occurs during oxygen reduction reaction at Au(100), the E_{eq} line for reaction (2) is calculated with $[HO_2^-]$ of 1 mM, in all other reactions the activity for species other than H^+,OH^- are assumed to be 1. In acidic environment, only reaction (1) is possible. For the 4e-ORR in alkaline solution ($pH^S \geq 11$), reaction (2) is the potential determining reaction, while reaction (4′) is the rate-determining step, whose thermodynamic potential is significantly upper shifted due to the strong adsorption of O_2^- at Au(100).

TOC

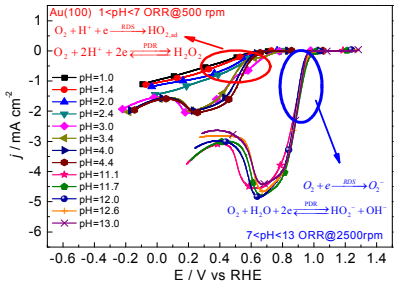

TOC text: The potential determining reaction and the rate-determining step for ORR at Au(100) in acid and alkaline solution have been clarified.